Inorg. Chem. **1984**, *23*, 1107–1113 **1107**

carried out on the University of Virginia laser facility purchased in part through National Science Foundation Grant No. CHE 77-09296.

Registry No. Ru(Me$_4$phen)$_3^{2+}$, 64894-64-0; Ru(4,7-Me$_2$phen)$_3^{2+}$, 24414-00-4; Ru(Me$_2$bpy)$_3^{2+}$, 32881-03-1; Ru(5,6-Me$_2$phen)$_3^{2+}$, 14975-40-7; Ru(Me-phen)$_3^{2+}$, 14975-39-4; Ru(phen)$_3^{2+}$, 22873-66-1; Ru(bpy)$_3^{2+}$, 15158-62-0; Ru(Cl-phen)$_3^{2+}$, 47860-47-9; Ru(Br-phen)$_3^{2+}$, 66908-45-0; HgCl$_2$, 7487-94-7; HgCl$_3^-$, 14988-07-9; HgCl$_4^{2-}$, 14024-34-1.

Contribution from the Departments of Chemistry, University of Virginia, Charlottesville, Virginia 22901, and James Madison University, Harrisonburg, Virginia 22807

Electron-Transfer Quenching of Ruthenium(II) Photosensitizers by Mercury(II) Chlorides. 2. Reactions in Aqueous Sodium Lauryl Sulfate Micellar Solutions

W. J. DRESSICK,[†] B. L. HAUENSTEIN, JR.,[†] J. N. DEMAS,*[†] and B. A. DEGRAFF*[‡]

Received August 19, 1983

Excited-state interactions of tris(α-diimine)ruthenium(II) photosensitizers with HgCl$_x^{2-x}$ (x = 2, 3, 4) were studied in the presence of sodium lauryl sulfate micelles. The results are compared with those of our previous study on the surfactant-free systems. The photosensitizers are tightly bound to the micelles, and the quenchers appear to be entirely in the aqueous phase, which radically modifies the quenching behavior. Equilibrium constants for formation of HgCl$_3^-$ and HgCl$_4^{2-}$ were evaluated by luminescence methods. Quenching proceeds via oxidative electron transfer to yield Ru(III) and Hg(I) free radicals. The failure to detect efficient ejection of anionic Hg(I) radicals from the anionic micelles is attributed to very fast reactions of the type $HgCl_2^-\cdot \rightarrow HgCl\cdot + Cl^-$. Marcus electron-transfer theory is modified to account for the differences between the micellar and homogeneous cases. HgCl$_2$ and HgCl$_3^-$ exhibit large inherent barriers to electron transfer ($\Delta G^*(0)$). Marcus theory permits evaluation of the otherwise unmeasurable redox potentials for the reaction Hg(II) + e$^-$ → Hg(I); the values are estimated to be ~−0.80 V, which agree with the values in surfactant-free media.

Introduction

We recently began investigating the excited-state reactivity of tris(α-diimine)ruthenium(II) complexes and mercury(II) species. We have described the quenching of a series of structurally and electronically similar $^*[RuL_3]^{2+}$ complexes (L = 2,2′-bipyridine, 1,10-phenanthroline, and their substituted derivatives) by Hg^{2+}[1] and by HgCl$_x^{2-x}$ (x = 2, 3, 4) in aqueous solution.[2] Quenching occurs by electron transfer. With Hg^{2+} the redox products, Hg$_2^{2+}$ and the Ru(III) complex, are formed with high efficiency. The back-reaction between the Ru(III) species and Hg$_2^{2+}$ is relatively slow (<10 M^{-1} s^{-1}) and provides an energy trap which forms the basis of a photogalvanic cell.[1]

We expected HgCl$_2$ to be superior to Hg^{2+} for solar energy storage because one of the anticipated final products, Hg$_2$Cl$_2$, should be insoluble and therefore slow the thermal back-reaction even further. For the HgCl$_x^{2-x}$ quenchers in fluid solution, however, no redox products have been observed even under flash photolysis conditions.[2] The main problem appears to be one of separation of the initial photoproducts

$$^*D + HgCl_2 \rightarrow {}^*D|HgCl_2 \rightarrow D^+|HgCl_2^- \tag{1a}$$

$$D^+|HgCl_2^- \rightarrow D|HgCl_2 \rightarrow D + HgCl_2 \tag{1b}$$

$$D^+|HgCl_2^- \rightarrow D^+ + HgCl_2^-\cdot \tag{1c}$$

where D denotes the Ru(II) photosensitizer and the encounter pairs are denoted by "|". Apparently, the dissociation step for the electrostatically stabilized pair D$^+$|HgCl$_2^-$ (eq 1c) is much slower than the energetically favorable back electron-transfer reaction (eq 1b). Any modifications that accelerate the separation of the redox partners in eq 1c would improve the yield of energetically valuable products.

One approach for assisting separation of the initial photoproducts is the use of charged micelles.[3,4] In our current system, an anionic micelle binds the Ru(II) photosensitizer, but the charge does not impede the approach of neutral HgCl$_2$. Following electron transfer, however, the negatively charged HgCl$_2^-$ should be ejected from the micelle, and the back-reaction should then be impeded by the electrostatic barrier. In addition to the possibility of enhancement of product separation, fundamental photochemical studies in micellar systems are inherently interesting because surfactants can enormously influence the nature and rates of reactions.[3,4]

We present here our study of the photochemical interactions of HgCl$_x^{2-x}$ (x = 2, 3, 4) and [RuL$_3$]$^{2+}$ photosensitizers in aqueous micellar NaLS solutions. We chose the relatively well-understood anionic surfactant sodium lauryl sulfate (NaLS) for study. The results are compared with those of our preceding study of the same systems in surfactant-free media,[2] and a model is developed to describe the effects introduced by the micelles. The model is also used in conjunction with Marcus electron-transfer theory to explain the quenching behavior for different Hg(II) species. Finally, the feasibility of the aqueous and micellar systems as solar energy converters is examined.

Experimental Section

The ruthenium(II) complexes used in this study and their preparation, purification, and characterization were described in the pre-

---

[†] University of Virginia.

[‡] James Madison University.

(1) DeGraff, B. A.; Demas, J. N. *J. Am. Chem. Soc.* **1980**, *102*, 6169.

(2) Hauenstein, B. L., Jr.; Mandal, K.; Demas, J. N.; DeGraff, B. A. *Inorg. Chem.*, preceding paper in this issue.

(3) (a) Fendler, J. H.; Fendler, E. J. "Catalysis in Micellar and Macromolecular Systems"; Academic Press: New York, 1975. (b) Holt, S. L., Ed. "Inorganic Reactions in Organized Media"; American Chemical Society: Washington, DC, 1982; ACS Symp. Ser. No. 177.

(4) (a) Grätzel, M. *Acc. Chem. Res.* **1981**, *14*, 376. (b) Grätzel, M.; Kalyanasundaram, K.; Kiwi, J. *Struct. Bonding (Berlin)* **1982**, *49*, 37. (c) Grätzel, M. *ACS Symp. Ser.* **1982**, *No. 177*, 113. (d) Yekta, A.; Aikawa, M.; Turro, N. *J. Chem. Phys. Lett.* **1979**, *63*, 543. (e) Ziemiecki, H.; Cherry, W. R. *J. Am. Chem. Soc.* **1981**, *103*, 4479. (f) Turro, N. J.; Grätzel, M.; Braun, A. M. *Angew. Chem., Int. Ed. Engl.* **1980**, *19*, 675. (g) Infelta, P. P.; Grätzel, M.; Thomas, J. K. *J. Phys. Chem.* **1974**, *78*, 191.

0020-1669/84/1323-1107$01.50/0

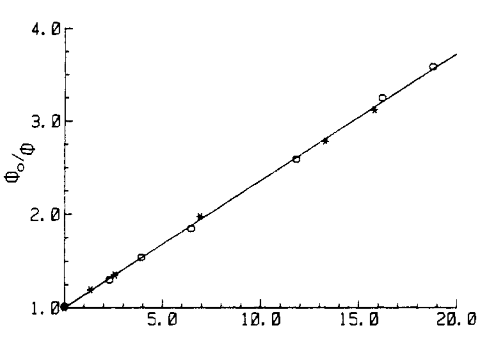

Figure 1. Lifetime (*) and intensity (○) Stern–Volmer plot of $HgCl_2$ quenching of $[Ru(Me_4phen)_3]^{2+}$ in 10 mM NaLS ($[HNO_3]$ = 0.01 M; 0.10 M $NaNO_3$ added).

ceding paper.[2] We used one additional complex in this study, $[Ru(4,7\text{-}(C_6H_5)_2phen)_3]^{2+}$ (abbreviated $[Ru(Ph_2phen)_3]^{2+}$).[5] Sodium lauryl sulfate (NaLS), Electrophoresis Purity Grade from Bio-Rad Laboratories, was purified by recrystallizing from methanol and vacuum-drying.

For the luminescence studies typical NaLS concentrations were 10 mM, which corresponds to a micelle concentration of $>3 \times 10^{-5}$ M.[6] The Ru(II) complex concentrations were $<1 \times 10^{-5}$ M, to ensure that the micelle occupancy number did not exceed unity.[7] For all experiments, 10 mM HNO_3 was present to prevent hydrolysis of the mercury complexes.

The differential pulse polarograms of the aqueous and micelle-bound $[Ru(bpy)_3]^{2+}$ were obtained at room temperature (23 ± 2 °C) with a PAR Model 174A Waveform Programmer. HNO_3 (0.15 M) was used as the supporting electrolyte. The complex concentration was 0.5 mM to provide adequate signal. For the micelle experiment, the NaLS concentration was 0.05 M, to ensure that the photosensitizer occupancy number was less than unity. The working and auxiliary electrodes were glassy carbon and platinum, respectively, and the reference electrode was a saturated calomel electrode (SCE).

Luminescence, lifetime, and flash photolysis measurements were made on the equipment described previously.[2] However, because we now appreciated the photosensitivity of the Br-phen complex, the laser was used in the single-shot mode, and the sample exposure was minimized. Lifetime decays were exponential over at least 2 half-lives. Stern–Volmer constants for $HgCl_2$ quenching ($K_{SV}(HgCl_2)$) at 0.00, 0.10, and 0.40 M $NaNO_3$ were determined from linear fits of $\tau_0/\tau - 1$ vs. $[HgCl_2]$. In all cases, the plots were linear within experimental error.

Stern–Volmer constants for $HgCl_3^-$ and $HgCl_4^{2-}$ ($K_{SV}(HgCl_3^-)$ and $K_{SV}(HgCl_4^{2-})$) were determined from simplex fits to titration data sets of two types. In both methods, the mercury was introduced as $HgCl_2$, which under our conditions means that the concentrations of Hg^{2+} and $HgCl^+$ are negligible. For $[Ru(phen)_3]^{2+}$ and $[Ru(4,7\text{-}Me_2phen)_3]^{2+}$, titrations were carried out at constant 0.40 M ionic strength and mercury(II) concentration, and $[Cl^-]$ was varied from 0.0 to 0.40 M by substitution of NaCl for $NaNO_3$.[2] Also, $K_{SV}(HgCl_3^-)$ and $K_{SV}(HgCl_4^{2-})$ were determined for all of the complexes by $HgCl_2$ titrations at 0.10 M NaCl. Details of the data fitting are given in Results.

Results

Figure 1, a typical Stern–Volmer plot, is for $[Ru(Me_4phen)_3]^{2+}$ in 10 mM NaLS, 10 mM HNO_3, and 0.10 M added $NaNO_3$. The data are linear within experimental error. The collinearity of the lifetime and intensity quenching plots indicates an absence of static quenching; all quenching is dynamic. $K_{SV}(HgCl_2)$'s, τ_0's, quenching constants ($k_q = K_{SV}/\tau_0$), and photosensitizer excited-state reduction potentials are presented in Table I.

Table I. Excited-State Reduction Potentials, τ_0, and Quenching Rate Constants for a Series of $[RuL_3]^{2+}$ Complexes Quenched by $HgCl_2$

L	$*E°$,[a] V	τ_0, μs	K_{SV},[b] M^{-1}	$10^{-6}k_q$, $M^{-1}\ s^{-1}$
Me_4phen	−1.11	1.85	139 ± 4	74.8 ± 6.0
4,7-Me_2phen	−1.01	3.30	100 ± 5	30.4 ± 2.4
Me_2bpy	−0.94	0.56	10.4 ± 0.7	18.8 ± 2.3
5,6-Me_2phen	−0.93	3.08	51.4 ± 4.6	16.7 ± 2.0
Me-phen	−0.90	2.26	29.8 ± 2.0	13.2 ± 1.7
Ph_2phen	−0.90	5.79	5.5 ± 0.8	0.95 ± 0.18
phen	−0.87	1.82	21.3 ± 2.0	11.7 ± 1.4
bpy	−0.84	0.78	3.0 ± 0.5	3.79 ± 0.83
Cl-phen	−0.77	2.08	5.1 ± 0.6	2.45 ± 0.34
Br-phen	−0.76	2.16	6.2 ± 0.9	2.88 ± 0.55

[a] Taken from ref 9a. [b] Values were determined in N_2-deaerated aqueous sodium lauryl sulfate solutions: $[NaLS]_{tot} = [HNO_3]$ = 10 mM; [Ru(II)] = 10 μm; $[NaNO_3]$ = 0.0 M.

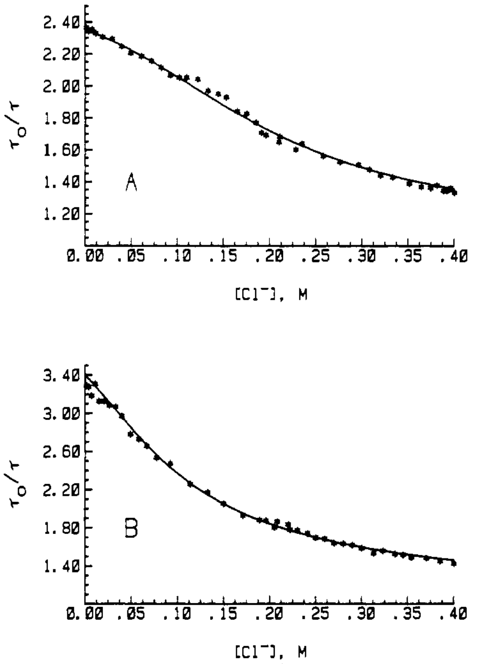

Figure 2. Chloride titrations of (A) $[Ru(phen)_3]^{2+}$ and (B) $[Ru(4,7\text{-}Me_2phen)_3]^{2+}$: (A) $[Hg(II)]_{tot}$ = 0.095 M introduced initially as $HgCl_2$; (B) $[Hg(II)]_{tot}$ = 0.030 M. In both experiments, [NaLS] = $[HNO_3]$ = 10 mM, and $[NaNO_3]$ + [NaCl] = 0.40 M. The asterisks represent the experimental points, and the solid lines are drawn with use of the parameters of Table II.

Figure 2 shows the variation of τ_0/τ at constant $[HgCl_2]$ vs. $[Cl^-]$ for $[Ru(phen)_3]^{2+}$ and $[Ru(4,7\text{-}Me_2phen)_3]^{2+}$. As in Part 1[2] we assume that this variation can be explained on the basis of reactions between $HgCl_2$ and Cl^-:

$$HgCl_2 + Cl^- \rightleftharpoons HgCl_3^- \quad K_3 \tag{2a}$$

$$HgCl_3^- + Cl^- \rightleftharpoons HgCl_4^{2-} \quad K_4 \tag{2b}$$

Clearly the nature of the Hg(II) quencher influences the rate of the quenching reaction. The order of reactivity is $HgCl_2 > HgCl_3^- > HgCl_4^{2-}$. Data were fit on the basis of

$$\tau_0/\tau = 1 + \sum(K_{SV}(HgCl_x^{2-x}))[HgCl_x^{2-x}] \tag{3a}$$

$$K_{SV}(HgCl_x^{2-x}) = (k_q(HgCl_x^{2-x}))\tau_0 \tag{3b}$$

where k_q is the quenching constant for the indicated species, τ_0 is the unquenched photosensitizer lifetime, and the summation is over x = 2–4.

At 0.40 M added electrolyte, the K_{SV}'s for $HgCl_3^-$ and $HgCl_4^{2-}$ for $[Ru(phen)_3]^{2+}$ and $[Ru(4,7\text{-}Me_2phen)_3]^{2+}$ were

---

(5) Watts, R. J.; Crosby, G. A. *J. Am. Chem. Soc.* **1971**, *93*, 3184.

(6) The micelle concentration is calculated from [M] = ([S] − CMC)/N, where [M] = micelle concentration, [S] = total surfactant concentration, CMC = critical micelle concentration, and N = aggregation number. For NaLS, CMC ≤ 8.1 mM and N = 62 (ref 3a, p 21), so 10 mM NaLS corresponds to $\geq 3.2 \times 10^{-5}$ M micelles.

(7) Poisson statistics govern the occupancy number of a micelle when the ratio of solute to micelle is less than 5.[4f]

Table II. Excited-State Reduction Potentials, τ_0, and Quenching Rate Constants for a Series of $[RuL_3]^{2+}$ Complexes Quenched by $HgCl_2$ and $HgCl_3^-$

			$HgCl_2$		$HgCl_3^-$	
L	$*E°$,[a] V	τ_0, μs	K_{SV},[b] M^{-1}	$10^{-6}k_q$, $M^{-1}\ s^{-1}$	K_{SV},[b] M^{-1}	$10^{-6}k_q$, $M^{-1}\ s^{-1}$
phen	−0.87	1.99	14.2 ± 1	7.14 ± 0.5	11.8 ± 1	5.93 ± 0.5
4,7-Me_2phen	−1.01	3.49	80.0 ± 4	22.9 ± 1.2	63.4 ± 4	18.2 ± 1.2

[a] Taken from ref 9a. [b] Values were determined in N_2-deaerated aqueous sodium lauryl sulfate solutions: $[NaLS]_{tot} = [HNO_3] = 10$ mM; [Ru(II)] = 10 μM; $[NaNO_3] + [NaCl] = 0.40$ M.

Table III. Excited-State Reduction Potentials, τ_0, and Quenching Rate Constants for a Series of $[RuL_3]^{2+}$ Complexes Quenched by $HgCl_2$ and $HgCl_3^-$

			$HgCl_2$		$HgCl_3^-$	
L	$*E°$,[a] V	τ_0, μs	K_{SV},[b] M^{-1}	$10^{-6}k_q$, $M^{-1}\ s^{-1}$	K_{SV},[b] M^{-1}	$10^{-6}k_q$, $M^{-1}\ s^{-1}$
Me_4phen	−1.11	2.19	133 ± 9	60.9 ± 5.5	57.8 ± 8	26.0 ± 4.4
4,7-Me_2phen	−1.01	3.36	80.4 ± 5	24.0 ± 2.4	38.5 ± 7	11.5 ± 2.4
Me_2bpy	−0.94	0.56	6.8 ± 0.7	12.0 ± 1.8	3.2 ± 0.8	5.78 ± 1.62
5,6-Me_2phen	−0.93	3.19	39.9 ± 3	12.5 ± 1.2	12.1 ± 2	3.79 ± 0.72
Me-phen	−0.90	2.44	25.6 ± 2	10.5 ± 1.0	8.2 ± 2	3.36 ± 0.91
Ph_2phen	−0.90	5.83	4.6 ± 0.3	0.80 ± 0.08	*c*	*c*
pheh	−0.87	1.80	12.9 ± 1	7.16 ± 0.91	7.7 ± 2	4.32 ± 1.22
bpy	−0.84	0.77	1.4 ± 0.3	1.84 ± 0.26	<0.10	<0.06 ± 0.03
Cl-phen	−0.77	2.20	3.2 ± 0.2	1.44 ± 0.15	<0.20	<0.09 ± 0.03
Br-phen	−0.76	2.20	2.5 ± 0.2	1.14 ± 0.55	1.0 ± 0.4	0.45 ± 0.20

[a] Taken from ref 9a. [b] Values were determined in N_2-deaerated aqueous sodium lauryl sulfate solutions: $[NaLS]_{tot} = [HNO_3] = 10$ mM; [Ru(II)] = 10 μM; $HgCl_2$ values were determined with $[NaNO_3] = 0.10$ M; $HgCl_3^-$ values were determined with [NaCl] = 0.10 M (see text for explanation of method). [c] Complex precipitated in the presence of Cl^-.

determined from a single simplex fit. The six variables used were K_3, K_4, $K_{SV}(HgCl_3^-)$, and $K_{SV}(HgCl_4^{2-})$ for $[Ru(phen)_3]^{2+}$ and $K_{SV}(HgCl_3^-)$ and $K_{SV}(HgCl_4^{2-})$ for $[Ru(4,7\text{-}Me_2phen)_3]^{2+}$. $K_{SV}(HgCl_2)$ values were determined from Stern–Volmer plots with 0.40 M $NaNO_3$ and no added chloride. The values of K_3 and K_4 were 44.5 and 9.87 M^{-1}, respectively. τ_0's, K_{SV}'s, and k_q's are presented in Table II. The theoretical curves determined from these parameters are shown by the solid lines in Figure 2. Residual plots of the differences between experimental and calculated data are random with respect to sign and magnitude, and the errors are well within our instrumental accuracy.

A plot of τ_0/τ vs. $[HgCl_2]$ with 0.10 M Cl^- added is shown in Figure 3. The nonlinear Stern–Volmer plots reflect the changing nature of the quenchers in the solution. At large $[Cl^-]/[HgCl_2]$, the higher chloromercury species dominate the solution composition. The observed τ_0/τ's are smaller than expected on the basis of the added $HgCl_2$ since $HgCl_2$ is the best quencher. As the amount of $HgCl_2$ added is increased and $[Cl^-]/[HgCl_2]$ decreases, less $HgCl_4^{2-}$ and progressively more $HgCl_3^-$ and $HgCl_2$ are present. τ_0/τ then more closely approaches the value expected for pure $HgCl_2$.

The K_{SV}'s determined at 0.10 M Cl^- were calculated as follows. An initial simplex fit was made to the τ_0/τ vs. $[HgCl_2]$ data simultaneously for all complexes with τ_0/τ's > 2 (i.e. $[Ru(phen)_3]^{2+}$, $[Ru(Me\text{-}phen)_3]^{2+}$, $[Ru(5,6\text{-}Me_2phen)_3]^{2+}$, $[Ru(4,7\text{-}Me_2phen)_3]^{2+}$, and $[Ru(Me_4phen)_3]^{2+}$). The variables were $K_{SV}(HgCl_3^-)$ and $K_{SV}(HgCl_4^{2-})$ for each complex and a common K_3 and K_4. The $K_{SV}(HgCl_2)$'s were determined from $HgCl_2$ quenching plots in the absence of added Cl^-. K_3 and K_4 (28.6 and 4.10 M^{-1}) obtained from this fit were then used to individually refit the titration curves for each complex with $K_{SV}(HgCl_3^-)$ and $K_{SV}(HgCl_4^{2-})$ as the fitting parameters. We estimate the K_3 and K_4 to be accurate to ~±30%. In all cases the resultant Stern–Volmer constants yielded calculated titration curves that matched the experimental data within experimental error; see Figure 3. Table III summarizes the Stern–Volmer quenching constants and the quenching rate constants determined with 0.10 M added Cl^-. $K_{SV}(HgCl_4^{2-})$ was substantially less than unity in all cases and was omitted from the table.

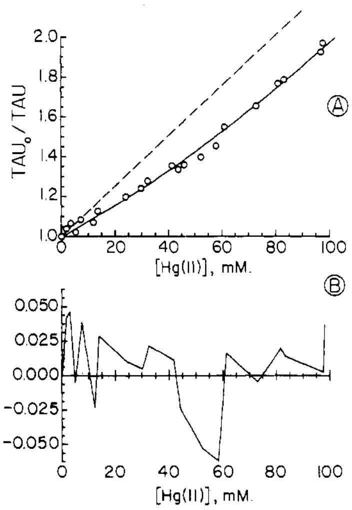

Figure 3. $HgCl_2$ titration of $[Ru(phen)_3]^{2+}$ with a fixed 0.10 M added NaCl concentration ($[NaLS] = [HNO_3] = 10$ mM). The experimental points are represented by open circles. The solid line is the best fit curve based on the Stern–Volmer constants of Table III. The dashed line shows the observed behavior if $NaNO_3$ replaced NaCl.

In an attempt to observe binding of $HgCl_2$ to the micelles, we determined K_{SV} for $[Ru(Me_4phen)_3]^{2+}$ as a function of [NaLS]. Within experimental error, there was no change in K_{SV} with [NaLS] (10–28 mM). This result indicates a very weak (<100 M^{-1}) or negligible binding of the quencher to the micelles.[4e]

The plots of log k_q vs. the excited-state reduction potential ($E°(Ru^{3+/*2+})$) are shown in Figure 4. Data for $HgCl_4^{2-}$ are omitted since the K_{SV}'s are too small to be measured accurately. The solid lines represent our best fits of the phenanthroline complexes using the Marcus–Weller theory (see Discussion).

Flash photolysis studies were carried out with use of $[Ru(phen)_3]^{2+}$ in 10 mM HNO_3 and 10 nmM NaLS. In the absence of NaLS there is a weak transient bleaching of the Ru(II) absorption spectrum which is independent of the presence of mercury(II) species. In the presence of NaLS,

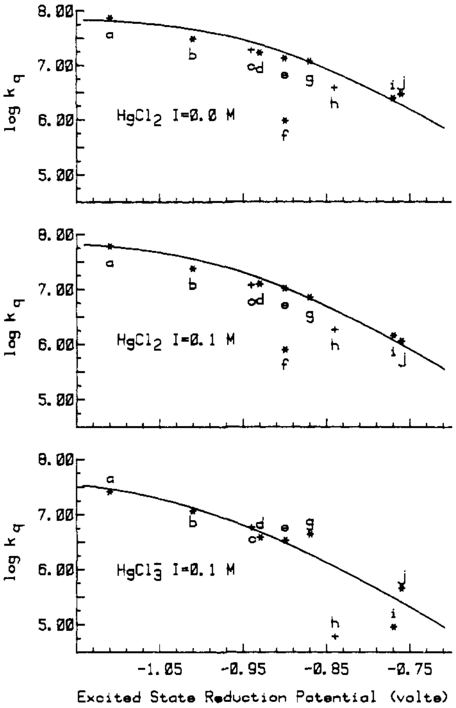

Figure 4. Weller plots of log k_q vs. $E°(D^+/^*D)$ with [NaLS] = [HNO_3] = 10 mM. The top and middle plots are for $HgCl_2$ quencher. The top plot is without added $NaNO_3$, and the middle plot is with 0.1 M $NaNO_3$. The bottom plot is for an $HgCl_3^-$ quencher with 0.10 M NaCl added. Letters identify experimental points for the following complexes: (a) $[Ru(Me_4phen)_3]^{2+}$; (b) $[Ru(4,7\text{-}Me_2phen)_3]^{2+}$; (c) $[Ru(Me_2bpy)_3]^{2+}$; (d) $[Ru(5,6\text{-}Me_2phen)_3]^{2+}$; (e) $[Ru(Me\text{-}phen)_3]^{2+}$; (f) $[Ru(Ph_2phen)_3]^{2+}$; (g) $[Ru(phen)_3]^{2+}$; (h) $[Ru(bpy)_3]^{2+}$; (i) $[Ru(Cl\text{-}phen)_3]^{2+}$; (j) $[Ru(Br\text{-}phen)_3]^{2+}$. The bipyridine complexes are denoted by plus signs and the phenanthroline ones by asterisks.

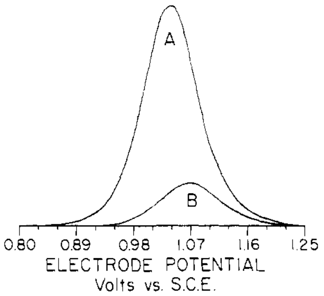

Figure 5. Differential pulse polarograms of $[Ru(bpy)_3]^{2+}$ in aqueous (A) and 50 mM NaLS (B) solution. [Ru(II)] = 0.50 mM; 0.15 M HNO_3 was added as the supporting electrolyte. The scan rate was 2 mV/s with a 10-mV modulation voltage.

however, there was a small and reproducible difference between solutions with and without $HgCl_2$. In the presence of 100 mM $HgCl_2$ the transient bleaching of the Ru(II) spectrum was somewhat greater and the decay to the base line was slower. We suggest that these differences are due to product separation and that the back reaction between Ru(III) and Hg(I) species is slowed by the presence of the NaLS micelle. The effect, however, is disappointingly small and represents a quantum efficiency for product separation well below 1%.

Figure 5 shows a differential pulse polarogram of $[Ru(bpy)_3]^{2+}$ in both aqueous and micellar solutions. At equal Ru(II) concentrations, the maximum peak current decreases nearly 5-fold on proceeding from the aqueous solution to the micellar environment. This decrease is accompanied by a slight anodic shift in E_p and a broadening of the wave. In aqueous solution, $E_{1/2}(Ru^{3+/2+})$ = 1.042 ± 0.003 V vs. SCE and the full width at half-maximum (fwhm) for the wave is 93 ± 2 mV.[8] These observations are in agreement with the known reversible behavior in aqueous solution.[9,10] In the micelle solution, $E_{1/2}(Ru^{3+/2+})$ = 1.075 ± 0.005 V vs. SCE and the fwhm is 112 ± 4 mV. In one experiment the Ru(II) concentration was reduced 10-fold at constant [NaLS]; the maximum peak current also decreases 10-fold while fwhm and $E_{1/2}(Ru^{3+/2+})$ remain unchanged.

The broadening of the wave in the micelle environment may be attributed to either of two effects: (i) irreversible charge transfer in the electrode oxidation or (ii) reversible charge transfer from a distribution of Ru(II)–micelle states. In case ii, the observed wave is the sum of the reversible waves for the oxidation of Ru(II) at the different micelle binding sites. We have no direct evidence for the validity of case ii. However, the absence of noticeable decomposition of the complexes in the quenching experiments and the reversibility noted in the systems during flash photolysis experiments suggest that case i is unlikely.

Discussion

We begin by considering the location of the sensitizers and quenchers in our system and the details of the quenching processes. Meisels et al.[11] have shown that $[Ru(bpy)_3]^{2+}$ is strongly bound to NaLS micelles. More recently, studies in this laboratory confirm this result for a variety of Ru(II) photosensitizers.[12] Further, a comparison of the K_{SV}'s for surfactant-free media[2] and the current data shows that the K_{SV}'s are reduced by typically 2–3 orders of magnitude. This demonstrates that at most ~1% of the photosensitizer can be free in solution. Thus, we eliminate the possibility that the photosensitizers have significant bulk solution concentrations. There are a number of quenching mechanisms for micelle-bound photosensitizers.[4]

In considering the details of our current system, we can promptly discount the possibility that quenching arises from release of the excited sensitizer into the bulk solution, where it is quenched by the Hg(II) species. With our observed quenching rate constants in the bulk solution,[2] every escaping photosensitizer would be quenched. Under these conditions quenching becomes limited by the escape rate and is independent of quencher concentration.[4g] This is totally inconsistent with the linear Stern–Volmer quenching plots.

When the photosensitizer is strongly bound to the micelles, there are four possible combinations of quencher location and quenching mechanism. These include either static or dynamic quenching on the micelle coupled with partial or complete binding of the quencher to the micelles. Lifetime and intensity quenching studies permit differentiation between these models.[4d]

Binding of $HgCl_2$ to the micelles seemed possible since Hg(II) forms complexes with oxygen donor ligands.[13] We

---

(8) (a) For differential pulse polarography, the criterion for reversibility in a one-electron transfer is an fwhm of 90.4 mV (in the limit of zero modulation voltage). $E_{1/2}$ is determined from the sum of the peak voltage (E_p) and half the modulation voltage ($^1/_2\Delta E$).[8b] (b) Bard, A. J.; Faulkner, L. R. "Electrochemical Methods: Fundamentals and Applications"; Wiley: New York, 1980; pp 190–199.

(9) (a) Lin, C.-T.; Bottcher, W.; Chou, M.; Creutz, C.; Sutin, N. *J. Am. Chem. Soc.* **1979**, *98*, 6536. (b) Balzani, V.; Bolletta, M.; Gandolfi, M. T.; Maestri, M. *Top. Curr. Chem.* **1978**, *75*, 1.

(10) Nagle, J. Ph.D. Dissertation, The University of North Carolina, 1979.

(11) Meisels, D.; Matheson, M. S.; Rabani, J. *J. Am. Chem. Soc.* **1978**, *100*, 117.

(12) (a) Hauenstein, B. L., Jr.; Dressick, W. J.; Buell, S. L.; Demas, J. N.; DeGraff, B. A. *J. Am. Chem. Soc.* **1983**, *105*, 4251.

(13) (a) Groth, P.; Hassel, O. *Acta Chem. Scand.* **1964**, *18*, 1326. (b) Prasad, S.; Garg, V. N. *J. Indian Chem. Soc.* **1965**, *42*, 259. (c) Yuan, S. T.; Madan, S. K. *Inorg. Chim. Acta* **1972**, *6*, 463. (d) Tosata, M.; Soccarsi, L.; Cignitti, M.; Paolini, L. *Tetrahedron* **1973**, *29*, 1339. (e, Manay, S.; Tobias, R. S. *Inorg. Chem.* **1975**, *14*, 287.

(14) Measurements in this laboratory indicate that quenching of $[RuL_3]^{2+}$ by Cu^{2+} is greatly influenced by NaLS micelles, and a break in the quenching plot results at the saturation limit.[15]

(15) Snyder, S. W.; Demas, J. N., unpublished results.

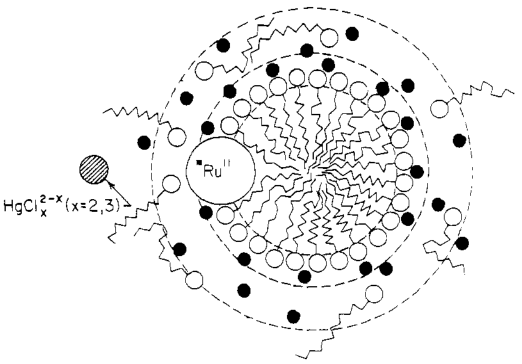

Figure 6. Representation of $[RuL_3]^{2+}$ imbedded in a micelle. Dashed lines represent the boundaries of (from the interior out): the inner core, the Stern layer, and the Gouy–Chapman layer. The solid circles are Na^+, and the open circles with tails are LS^-.

would, however, expect $HgCl_3^-$ and $HgCl_4^{2-}$ to exhibit less favorable binding interactions with the micelles due to steric and electrostatic effects. We found no spectroscopic evidence for the binding of $HgCl_2$. The excellent agreement between the intensity and lifetime Stern–Volmer plots of Figure 1 rules out any static quenching, and the absence of nonexponential decays for our conditions rules out complete micellization of the quencher. The linearity of the quenching plots at quencher concentrations exceeding the available binding sites (i.e. no more than one Hg species could be associated with each SO_4^- group) also argues against a completely micellized quencher. While we have been unable to compare intensity and lifetime quenching plots for $HgCl_3^-$, we assume that there is no static quenching because of electrostatic repulsion between this anion and the anionic micelle.

Partial micellization of the quencher can fit our results, but only in the limiting cases of negligible binding to the micelle or very poor intramicellar quenching. Any other situation would typically produce nonexponential decay curves, which we do not observe. Since $HgCl_2$ and $HgCl_3^-$ are good quenchers in homogeneous solutions, we conclude that they are only very weakly bound to the micelles. As added support for this weak-binding case we find no variation in $K_{SV}(HgCl_2)$ for $[Ru(Me_4phen)_3]^{2+}$ with [NaLS] (10–28 mM). This is only consistent with a very weak binding case[4e] with a binding constant of $<100\ M^{-1}$.

As we have no evidence for binding of our quenchers to the micelles and since we would not expect $HgCl_3^-$ to bind to anionic micelles at all, we adopt a different model than is traditionally given.[4] We assume that there is negligible binding of the quencher to the micelles. Then, since the charged photosensitizers are deactivated by water-borne quenchers, we assume that the sensitizers are bound to the surface of the micelles (Figure 6). The quenching rate is then determined by the rate of collision between solution quenchers and micellized sensitizer.

This model readily explains the relative reactivity of the $HgCl_x^{2-x}$ (x = 2, 3, 4) species. With the ruthenium complex bound to the micelle, the effective charge on the photosensitizer is negative.[16] On the basis of electrostatic arguments, the relative reactivity of the Hg(II) complexes should be $HgCl_2 > HgCl_3^- > HgCl_4^{2-}$, which is the observed reactivity.

In the preceding paper,[2] we show that quenching of $[RuL_3]^{2+}$ by $HgCl_x^{2-x}$ (x = 2, 3, 4) in surfactant-free media is by electron transfer. The Weller plots of Figure 4 exhibit the expected dependence on the driving force for electron-transfer quenching. We conclude from this result and by arguments given in Part I[2] that quenching in NaLS media is also by electron transfer.

The one complex that was not used in the aqueous study because of low solubility, $[Ru(Ph_2phen)_3]^{2+}$, shows unusually low reactivity in the NaLS micelle system. On the basis of its excited-state reduction potential, this complex should react at the same rate with $HgCl_2$ as $[Ru(Me\text{-}phen)_3]^{2+}$, but its observed reactivity is roughly 1 order of magnitude less. We have shown elsewhere, however, that micellized $[Ru(Ph_2phen)_3]^{2+}$ is significantly less exposed to the solvent than the remaining complexes used here.[12] We conclude that the low reactivity of $[Ru(Ph_2phen)_3]^{2+}$ is due to its reduced exposure to the solvent-borne quenchers. In subsequent discussion we do not include it with the rest of the phenanthroline complexes.

In the preceding paper, we explained the luminescence quenching of polypyridyl Ru(II) complexes by $HgCl_x^{2-x}$ (x = 2, 3, 4) using electron-transfer theory.[17–19] The basic model and the definition of terms were given.[2] We extend this treatment to the micellar systems, but the evaluations of k_{12}, k_{21}, k_{30}, and ΔG_{23} differ. We modify the relationships developed for homogeneous fluid solutions to reflect the nature of the micellar systems and obtain a simple and satisfactory description of these systems.

In homogeneous fluid solution, the diffusion-controlled reaction rate, k_{12}, is approximated by the Debye–Smoluchowski equation.[20] The Eigen equation may be used to estimate the precursor complex dissociation rate (k_{21}) in aqueous solution.[21] There are several problems that occur in attempting to apply these approximations here. First, it is difficult to obtain reliable estimates of the effective charge and radius of the micelles. Also, since the Debye–Smoluchowski and Eigen equations are strictly applicable only for point charges, the large size of the micelles strains these models.

One of the major problems that any model must address is the discrepancies between k_{12} estimated by the Debye–Smoluchowski equation and the observed data. For our micelles for $HgCl_2$, we calculate $k_{12} = 10^{10}\ M^{-1}\ s^{-1}$, which is orders of magnitude larger than the observed values. Even for the charged $HgCl_3^-$, electrostatic repulsion is inadequate for explaining the observed reductions in k_q.

Figure 6 shows an idealized representation of the micellar environment and illustrates one reason for the great reduction in k_q on binding to the micelles. Only a small fraction of the quenchers striking the micelle can interact successfully with the embedded Ru(II) complex. We can approximate the reduction in k_q compared to that expected from the micelle quencher collision rate by means of a hard-sphere geometric-shielding model. We assume that the complex is embedded in the micelle with only some fraction of it projecting into the solution. The probability that a quencher colliding with the micelle–sensitizer assembly will actually strike the photosensitizer is then given by the area that the sensitizer presents to the solution divided by the total surface area of the photosensitizer–micelle assembly. This geometric reduction factor A can be approximated by

---

[16] Fendler and Fendler[3a] indicated that the degree of dissociation of Na^+ from the micelle is ~20%. This degree of dissociation is inappropriate for our model since it represents the fraction of counterions completely dissociated from the micelle surface and from the Gouy–Chapman double-layer. Our model (vide infra) is based on the assumption that it is the degree of dissociation from the micelle surface alone that is significant since the quenching occurs at the micelle surface.

[17] (a) Marcus, R. A. *Annu. Rev. Phys. Chem.* **1964**, *15*, 155. (b) Sutin, N. In "Inorganic Biochemistry"; Eichorn, G., Ed.; Elsevier: Amsterdam, 1973; p 611. (c) Marcus, R. A. In "Tunneling in Biological Systems"; Chance, B., et al., Eds.; Academic Press: New York, 1979; p 109 and references therein.

[18] (a) Rehm, D.; Weller, A. *Ber. Bunsenges. Phys. Chem.* **1969**, *73*, 834. (b) Rehm, D.; Weller, A. *Isr. J. Chem.* **1970**, *8*, 259.

[19] Scandola, F.; Balzani, V.; Schuster, G. *J. Am. Chem. Soc.* **1981**, *103*, 2519.

[20] Debye, P. *Trans. Electrochem. Soc.* **1942**, *82*, 265.

[21] Eigen, M. *Z. Phys. Chem. (Wiesbaden)* **1954**, *1*, 176.

$$A = F(R_R/R_M)^2 \tag{4}$$

F is the fractional area of the sensitizer that is exposed to the aqueous solution, and R_R and R_M are the radii of the ruthenium complex and the micelle, respectively. Both the micelle and the complex are assumed to be spherical. For our complexes and micelles the A's calculated by eq 4 agree with the exact solution to better than 2%. We have previously evaluated F's for the complexes studied here.[12] If the Ph_2phen complex, which has a very low F, is ignored, the remaining F's were rather close to $^1/_3$, and we use this average value for all the data.[12] R_R is 8.4 Å, and estimates for R_M are 22–27 Å.[22] Using R_M = 25 Å, we find A = 0.0376. This means that geometric shielding reduces the effectiveness of encounters with the micelle by almost a factor of 30.

As in Part 1,[2] we are unable to estimate k_{30} in the absence of photochemistry. We assume that since the rate constant represents an intraencounter-pair value that it should be similar regardless of whether the complex is bound to a micelle or not; we, therefore, use the 2×10^{10} M^{-1} s^{-1} value used in Part 1.

ΔG_{23}, the free energy change for the electron transfer, is given by[19]

$$\Delta G_{23} = E°(D^+/{}^*D) - E°(A/A^-) + W_p - W_r \tag{5}$$

A problem arises if $E°(D^+/{}^*D)$ differs in the aqueous and micellar media. As shown in Figure 5, however, the oxidation potential for $[Ru(bpy)_3]^{2+}$ is shifted only slightly (~30 mV) on binding to micelles. Also, binding of the Ru(II) complexes to NaLS does not greatly affect the MLCT excited-state energies; the emission bands exhibit a red shift of <10 nm in 10 mM NaLS compared to the emission in water.[23] Therefore, we use the aqueous $E°(D^+/{}^*D)$'s in this work.[2] To minimize the number of fitting parameters, we have assumed that $E°(A/A^-)$ was unaffected by binding to the micelles and have used the value of −0.80 V obtained from the surfactant-free media.[2] Unlike the aqueous system, W_p and W_r are now significant because of the large micellar charge. In water, at 25 °C, W_p or W_r are given by[24]

$$W_p \text{ or } W_r = 0.185 Z_R Z_M\{1/[1 + 0.5aI^{1/2}]\}/a \tag{6}$$

where Z_M is the charge on the micellized ruthenium complex. Z_R is the charge on the Hg(II) quencher for W_r or on the Hg(I) photoproduct for W_p. I is the ionic strength in moles/L. a is the separation distance between the two reactants. We determined a from the sum of R_M and the radius of the appropriate Hg(II) species.[2] Although the assumption of point charges in the current case is not strictly valid because of the polarizability of the micelles, eq 6 should supply a reasonable estimate of W_p or W_r. Further, this term is small enough that any errors contributed to our final results by eq 6 will be minimal.

We estimated k_{21} in the same manner as described in part 1.[2] We assumed somewhat arbitrarily a micelle charge of 35– in all calculations. The use of larger micelle charges with the Debye–Smoluchowski equation will yield k_{12}'s that are less than the observed k_q's. A value of 15– has been estimated in the literature, but this value is too small for our model.[16] Because of the curvature of the Weller plots, k_{12} was estimated as part of the fitting parameters as was $\Delta G^{\ddagger}(0)$.

Table IV summarizes our results. The errors and uncertainties are estimated as in part 1.[2] The solid lines in Figure 4 represent the fitting obtained with use of the values in Table IV to fit the experimental data for the phenanthroline complexes. First, all of the data can be reasonably well fit with use of $E°(A/A^-)$ for the surfactant-free media. This indicates that $E°(A/A^-)$ is probably not greatly affected by the media. Also, Table IV shows that $\Delta G^{\ddagger}(0)$ appears to increase significantly on going to the micellar system.[2] While one may argue over the precise values of $\Delta G^{\ddagger}(0)$, the shapes of the Weller plots establish the presence of larger reorganizational energies for $HgCl_2$ and $HgCl_3^-$, which are not present in the corresponding aqueous systems.[2]

Table IV. Parameters Used in Fits to log k_q vs. $^*E°([RuL_3]^{2+})$ for Quenching by $HgCl_2$ at 0.00 M and 0.10 M Added $NaNO_3$ and $HgCl_3^-$ in 0.10 M NaCl Solution

	quencher		
	$HgCl_2$ 0.0 M $NaNO_3$	$HgCl_2$ 0.1 M $NaNO_3$	$HgCl_3^-$ 0.1 M NaCl
k_{12}, M^{-1} s^{-1}	8.0×10^7	8.0×10^7	1.0×10^8
k_{21}, s^{-1}	1.2×10^9	6.7×10^8	1.5×10^9
k_{30}, s^{-1}	2.0×10^{10}	2.0×10^{10}	2.0×10^{10}
k°_{23}, s^{-1}	1.6×10^{12}	1.6×10^{12}	1.6×10^{12}
$E°$(Hg(II/I)), V	−0.80 ± 0.1	−0.80 ± 0.1	−0.80 ± 0.1
W_r, V	0.000	0.000	0.038
W_p, V	0.068	0.038	0.073
$\Delta G^{\ddagger}(0)$, cal	7000 ± 500	7000 ± 500	7600 ± 500
$\Delta G^{\ddagger}(0)$, cal[a]		4700 ± 500	4300 ± 800

[a] Aqueous results; values determined at 1 M ionic strength.[2]

$\Delta G^{\ddagger}(0)$ is the energy necessary to reorganize the nuclear configurations of the precursor complex prior to electron transfer.[19] Our model describes a Ru(II) complex deeply embedded in the micelle with only a portion extending into the aqueous phase. The micelle environment is highly hydrophobic, and the work necessary to reorganize the media around the sensitizer to accommodate an increase in sensitizer change would be expected to be greater than for an analogous rearrangement in pure water. In part, the difference in $\Delta G^{\ddagger}(0)$ between the micellar and aqueous systems may be ascribed to this phenomenon.

Alternatively, micellar charge should influence the $\Delta G^{\ddagger}(0)$'s. To accomplish an electron transfer on the micelle, the charges on the reactants, especially the mercury quencher, would have to change in a large electrostatic gradient. The gradient would force the species to undergo large conformational changes to achieve their most stable forms, which would result in large $\Delta G^{\ddagger}(0)$'s as is observed here. In the surfactant-free media, however, these electrostatic contributions to the $\Delta G^{\ddagger}(0)$'s are smaller.[2]

Conclusions

From the current study we make several important observations:

(i) A simple hard-sphere model is developed, which accounts for the diminution of quenching constants on binding sensitizers to micelles when the quencher has negligible solubility in the micelle.

(ii) Marcus theory can be adapted to account for the differences in electron-transfer quenching behavior in micellar and homogeneous media.

(iii) The relative $\Delta G^{\ddagger}(0)$ values in aqueous and micellar solutions can be understood from the local environment of the electron transfer reaction. Large $\Delta G^{\ddagger}(0)$'s are expected when charge is changed in a hydrophobic environment and in the presence of large electrostatic gradients.

(iv) The expected electrostatic ejection of $HgCl_2^{-}\cdot$ from the micelle failed with these ruthenium complexes. A possible explanation is the reaction

$$HgCl_2^{-}\cdot \rightarrow HgCl\cdot + Cl^- \tag{7}$$

---

(22) Calculated from: Tanford, C. "The Hydrophobic Effect"; Wiley: New York, 1980; Chapter 8.

(23) Buell, S. L.; Snyder, S. W.; Demas, J. N., unpublished results.

(24) (a) Haim, A.; Sutin, N. *Inorg. Chem.* **1976**, *15*, 476. (b) Bock, C. R.; Connor, J. A.; Gutierrez, A. R.; Meyer, T. J.; Whitten, D. G.; Sullivan, B. P.; Nagle, J. K. *J. Am. Chem. Soc.* **1979**, *101*, 4815. (c) Chibisov, A. K. *Russ. Chem. Rev.* (*Engl. Transl.*) **1981**, *50*, 615.

which proceeds so rapidly that it cannot be followed even with pulse radiolysis.[25] If reaction 7 occurs prior to ejection of $HgCl_2^-$ from the micelle, the back-reaction between Ru(III) and HgCl· can compete effectively with the escape of the neutral radical. It is apparent that construction of micelle-based solar energy storage devices must consider processes other than the primary electron-transfer reaction.

Acknowledgment. We gratefully acknowledge support by the donors of the Petroleum Research Fund, administered by the American Chemical Society, the Air Force Office of Scientific Research (Grant No. 78-3590), and the NSF (Grant No. CHE 82-06279). We gratefully acknowledge discussions with S. L. Buell and J. R. Bacon, and we thank R. J. Sundberg for the loan of the electrochemical system. The University of Virginia laser facility was purchased in part with the NSF Grant No. CHE 77-09296.

Registry No. $[Ru(Me_4phen)_3]^{2+}$, 64894-64-0; $[Ru(4,7\text{-}Me_2phen)_3]^{2+}$, 24414-00-4; $[Ru(Me_2bpy)_3]^{2+}$, 32881-03-1; $[Ru(5,6\text{-}Me_2phen)_3]^{2+}$, 14975-40-7; $[Ru(Me\text{-}phen)_3]^{2+}$, 14975-39-4; $[Ru(Ph_2phen)_3]^{2+}$, 63373-04-6; $[Ru(phen)_3]^{2+}$, 22873-66-1; $[Ru(bpy)_3]^{2+}$, 15158-62-0; $[Ru(Cl\text{-}phen)_3]^{2+}$, 47860-47-9; $[Ru(Br\text{-}phen)_3]^{2+}$, 66908-45-0; $HgCl_2$, 7487-94-7; $HgCl_4^{2-}$, 14024-34-1; $HgCl_3^-$, 14988-07-9; NaLS, 151-21-3.

---

(25) Nazhat, N. B.; Asmus, K.-D. *J. Phys. Chem.* **1973**, *77*, 614.

Contribution from the Istituto di Chimica Generale ed Inorganica, Università di Roma, Rome, Italy, and Institut für Anorganische Chemie, Universität München, D-8000 München 2, FRG

He I and He II Photoelectron Spectra and Infrared Intensity Measurements of Alkynylmercury(II) Compounds: The Search for dπ–pπ Interactions

C. CAULETTI,*† C. FURLANI,† M. N. PIANCASTELLI,† A. SEBALD,‡ and B. WRACKMEYER‡

Received March 16, 1983

The UV photoelectron spectra of various alkynylmercury(II) compounds of the type $Hg(C\equiv CR)_2$ (I), $R'HgC\equiv CR$ (II), and $R'HgC\equiv CHgR'$ (III) are reported and discussed with regard to structural implications. The spectra provide evidence for significant dπ–pπ interactions only for compounds in which a conjugation extended along the molecular axis between the π-acetylenic orbitals and other π systems is possible, as is evident from ligand field effects on the 5d mercury orbitals. This is substantiated by IR intensity measurements of the $\nu_{C\equiv C}$ stretching band of compounds I and II. From the comparison of this information with NMR results, it appears that dπ–pπ interactions are weak in any case. In general, the trends of $\pi_{C\equiv C}^{-1}$, σ_{Hg-C}^{-1}, and d^{-1} ionizations are in agreement with changes in the magnitude of various NMR parameters ($\delta(^{13}C)$, $\delta(^{199}Hg)$, $J(Hg-C)$, $J(C\equiv C)$).

Introduction

For many transition metals, dπ–pπ interactions between d metal orbitals and π systems of organyl ligands are in general readily established by various methods.[1] This appears to be more difficult, for obvious reasons, in the case of organomercury compounds.

In a recent NMR study of alkynylmercury(II) compounds,[2] it proved impossible to present unambiguous evidence for this by ^{13}C NMR spectroscopy although it appears that the nuclear shielding of mercury is related to changes in the energy of the mercury 5d orbitals.

As far as other spectroscopic methods are concerned, the measurement of infrared (IR) intensities and, in particular, UV photoelectron spectroscopy (UPS) may help to assess the existence and the extent of dπ–pπ interactions.

The infrared intensities of $\nu_{C\equiv C}$ in alkynes are determined by resonance interactions of the C≡C triple bond with the substituents,[3] and the IR intensities of $\nu_{C\equiv N}$ and $\nu_{C\equiv O}$ in transition-metal compounds reflect metal–ligand dπ–pπ interactions.[4]

UPS enables observation of the shape and energy of the ionization of valence orbitals, particularly of the 5d mercury ionization, and of the bands related to π^{-1} organyl ionizations.[5]

The alkynylmercury(II) compounds that this paper deals with have been selected for several reasons: (i) extensive NMR data are available for comparison,[2] (ii) most of the compounds fulfill the criteria required for meaningful discussion of IR intensity data,[6] and (iii) previous work[5] on UPS of some bis(alkynyl)mercury(II) compounds shows that alkynyl ligands are suitable candidates to study dπ–pπ interactions.

In order to establish criteria that could be ultimately used to predict the extent of π interactions in organomercury compounds and similar classes of molecules, we extended our investigation to alkynylmercury(II) compounds of the types $Hg(C\equiv CR)_2$ (I: R = CH_3 (a), $n\text{-}C_4H_9$ (b), $t\text{-}C_4H_9$ (c), C_6H_5 (d), $p\text{-}CH_3OC_6H_4$ (e), Cl (f), Br (g)), $R'HgC\equiv CR$ (II: R = H, R′ = CH_3 (a), C_2H_5 (b), $CH{=}CH_2$ (c), C_6H_5 (d); R = R′ = CH_3 (e); R = C_6H_5, R′ = CH_3 (f); R = R′ = C_6H_5 (g)), and $R'HgC\equiv CHgR'$ (III: R′ = CH_3 (a), C_2H_5 (b), C_6H_5 (c)).

The NMR parameters (^1H, ^{13}C, ^{199}Hg) have been reported for compounds I–III[2] with the exception of Ig and IIe (see Experimental Section). IR intensities have been measured for compounds I, except for Ic (in Ic the C≡C stretching band occurs as two peaks, which is a common feature of disubstituted $t\text{-}C_4H_9$ alkynes and may be attributed to Fermi resonance with various bands[7]), and for compounds II, except for

---

† Università di Roma.
‡ Universität München.

(1) (a) Furlani, C.; Cauletti, C. *Struct. Bonding (Berlin)* **1978**, *35*, 119. (b) Kettle, S. F. A.; Paul, J. *Adv. Organomet. Chem.* **1972**, *10*. (c) Mann, B. E. *Ibid.* **1974**, *12*.

(2) Sebald, A.; Wrackmeyer, B. *Spectrochim. Acta, Part A* **1982**, *38A*, 163.

(3) (a) Grindley, T. B.; Johnson, K. F.; Katritzky, A. R.; Keogh, H. J.; Thirkettle, C.; Brownlee, T. T. C.; Munday, J. A.; Topsom, R. D. *J. Chem. Soc., Perkin Trans. 2* **1974**, 276. (b) Grindley, T. B.; Johson, K. F.; Katritzky, A. R.; Keogh, H. J. Thirkettle, C.; Topsom, R. D. *Ibid.* **1974**, 282.

(4) (a) Schlodder, R.; Vogler, S.; Beck, W. *Z. Naturforsch. B: Anorg. Chem., Org. Chem., Biochem., Biophys., Biol.* **1972**, *27B*, 463. (b) Jones, L. H. *Inorg. Chem.* **1963**, *2*, 777. (c) van Rentergem, M.; van der Kelen, G. P.; Claeys, E. C. *J. Mol. Struct.* **1982**, *80*, 317.

(5) Furlani, C.; Piancastelli, M. N.; Cauletti, C.; Faticanti, F.; Ortaggi, G. *J. Electron Spectrosc. Relat. Phenom.* **1981**, *22*, 309.

(6) (a) Davies M. "Infrared Spectroscopy and Molecular Structure"; Elsevier: Amsterdam, 1963. (b) Gans, P. "Vibrating Molecules"; Chapman and Hall, London 1975.

0020-1669/84/1323-1113$01.50/0